Research Article

Journal of Physical Organic Chemistry

Received: 25 February 2011, Revised: 6 May 2011, Accepted: 10 May 2011, Published online in Wiley Online Library: 19 July 2011

(wileyonlinelibrary.com) DOI 10.1002/poc.1894

Optoelectronic property tailoring of conjugated heterocyclic azomethines – the effect of pyrrole, thiophene and furans

Stéphane Dufresne[a] and W. G. Skene[a]*

A series of *de novo* symmetric heterocyclic azomethine dyads and triads consisting uniquely of furans, thiophenes, pyrroles and methyl-pyrroles were prepared. These were prepared to investigate the effect of various heterocycles and the degree of conjugation on the spectroscopic and electrochemical properties. The crystallographic structures of the symmetric azomethines were also compared with their unsymmetric and heterocyclic and homoaryl counterparts. It was found that for a similar series, bathochromic absorbance and fluorescence shifts occurred when progressing in the order of furan < thiophene < pyrrole ≈ methyl-pyrrole. The spectroscopic properties of the heterocyclic azomethines were also bathochromically shifted relative to their homoaryl analogues as a result of increased degree of conjugation and electronic effects. The former was in part confirmed by crystallographic studies showing the heterocycles adopted co-planar and antiparallel arrangements. Although all the compounds studied showed weak fluorescence at room temperature, their fluorescence could be restored at low temperatures, implying deactivation of the singlet excited manifold by bond rotation. Meanwhile, irreversible oxidation was observed for all the azomethines studied and their oxidation potentials were contingent on the heterocycle and number of azomethines, ranging between 0.8 and 1.4 V versus Ag^+. The irreversible oxidation was due to radical cation cross-coupling resulting in products with higher degrees of conjugation. Copyright © 2011 John Wiley & Sons, Ltd.
Supporting information may be found in the online version of this article.

Keywords: fluorescence; imines; physical properties; synthesis

INTRODUCTION

Conjugated materials have found uses in organic electronic devices including light emitting diodes, photovoltaics and field effect transistors.[1–3] This is partly because of their optoelectronic properties that are compatible with such devices. Although these materials are prepared from aryl–aryl coupling protocols, property enhancements resulting in increased device efficiencies are possible by incorporating vinylene linkages.[4,5] These unsaturated connecting units are understood to prevent rotation around the aryl–aryl bond leading to increased planarity. Despite the enhanced optoelectronic properties that are possible with vinylene derivatives, their preparation requires stringent reaction conditions.[6–8] Their preparation additionally produces substantial amounts of unwanted by-products relative to the desired products, requiring extensive purification for achieving optimal properties and device performance.

Azomethines (–N = CH–) are interesting alternatives to vinylene linkages in part owing to their straightforward preparation that does not require stringent reaction conditions.[9] Moreover, they are isoelectronic to their carbon counterparts.[10] Given the synthetic advantages of azomethines and their expected similar properties to their vinyl cousins, much work is still required for assessing their suitability for replacing functional materials currently used in organic electronic devices. Additional azomethine examples are further required to demonstrate that functional materials-like properties are possible with these heteroatomic conjugated systems, in contrast to the limited properties exhibited by previously investigated compounds.[11–14] This is of particular importance given that azomethines are generally accepted to be hydrolytically, oxidatively and reductively unstable in addition to being acid sensitive, precluding their use as functional materials in working devices.[15–17] Although some property improvements are possible with homoaryl azomethines,[11,18] their optoelectronic properties are not comparable to their vinylene analogues. This is a result of inherent twisting around the aryl–azomethine bonds that limits their degree of conjugation.[10,19–27] Enhanced azomethine optoelectronic properties comparable to their vinylene analogues are however possible with thiophene derivatives.[6,7,28,29] This is in part a result of coplanarization of the thiophene–azomethine moieties. This leads to higher degrees of conjugation relative to the homoaryl azomethines, resulting in delocalization of the heterocyclic electronic effects across the entire conjugated framework.

Although enhanced properties are possible with azomethines prepared exclusively with thiophenes, azomethines derived from other heterocycles are unknown and their optoelectronic properties remain unexplored.[30] In fact, to the best of our knowledge, there are no previous reports examining the

* *Correspondence to: W. G. Skene, Laboratoire de caractérisation photophysique des matériaux conjugués, Département de Chimie, Université de Montréal, CP 6128, Centre-ville, Montreal, QC, Canada.*
E-mail: w.skene@umontreal.ca

a *S. Dufresne, W. G. Skene*
Laboratoire de Caractérisation Photophysique des Matériaux Conjugués, Département de Chimie, Université de Montréal, CP 6128, Centre-ville, Montreal, QC, Canada

preparation and structure/property studies of azomethines consisting uniquely of heterocycles. We therefore were interested in investigating the effect of different heterocycles and symmetric and unsymmetric azomethines consisting entirely of heterocycles on the photophysical and electrochemical properties. This is of particular interest for gaining an important understanding of azomethine structure/property relationships and for the design and preparation of new functional materials with enhanced properties for potential use in devices. To this means, dyad and triad model compounds (Chart 1) consisting of one and two azomethines, respectively, were prepared by condensing furans, pyrroles and thiophenes monoaldehydes with aminothiophenes (**1** and **2**). *De novo* symmetric azomethines were prepared and their optoelectronic properties were compared with their unsymmetric derivatives in addition to their corresponding homoaryl counterparts for examining the possibility of optoelectronic property tailoring. In particular, the absorbance, fluorescence and fluorescence quantum yields contingent on azomethine structure were examined. The preparation, photophysical and electrochemical properties of these conjugated heterocyclic azomethines in addition to their crystallographic data are herein presented to illustrate the enhanced properties possible with these conjugated heteroatom and all-heterocyclic compounds.

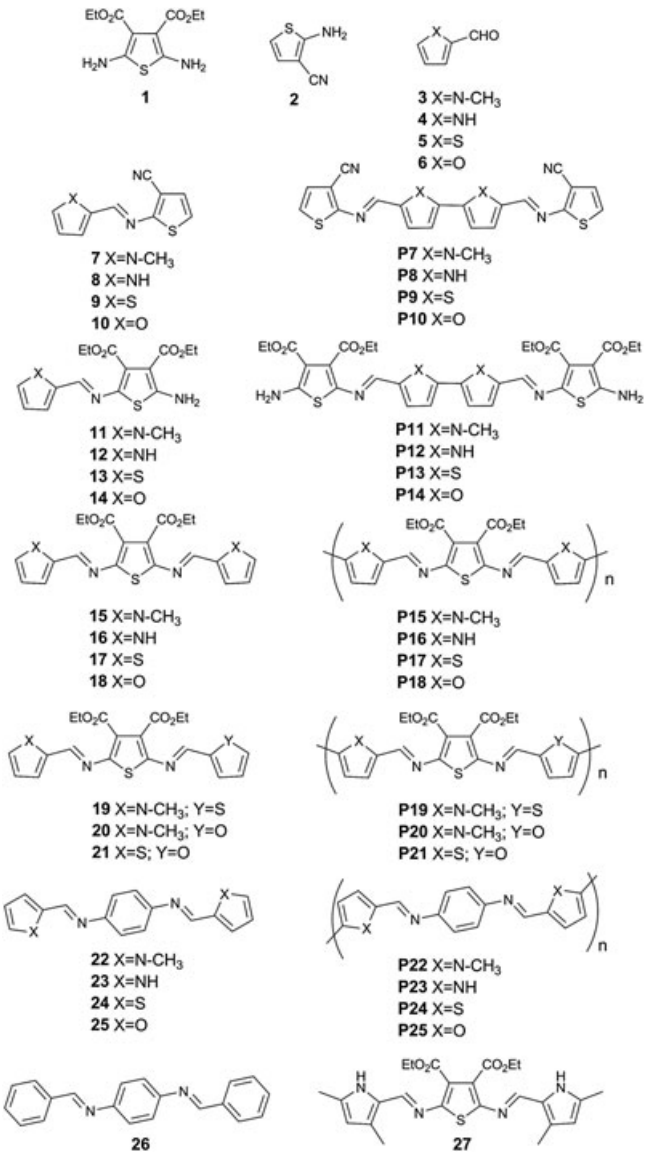

Chart 1. Heterocyclic azomethines, representative homoaryl analogues and anodically coupled products prepared and investigated

EXPERIMENTAL SECTION

Materials and general methods

All chemicals were commercially available from Aldrich (Oakville, ON, Canada) including **3–6** and were used as received unless otherwise stated. Anhydrous and deaerated solvents were obtained with a Glass Contour (Irvine, CA, USA) solvent purification system. NMR spectra were recorded on a Bruker (Milton, ON, Canada) 400 MHz spectrometer with the appropriate deuterated solvents.

Spectroscopic methods

The absorption measurements were done on a Varian Cary-500 spectrometer (Dorval, QC, Canada) while the fluorescence studies were performed on an Edinburgh Instruments FLS-920 fluorimeter after deaerating the samples thoroughly with nitrogen for 20 min with NSG Precision Cells (Farmingdale, NY, USA) cuvettes. Fluorescence quantum yields were measured with samples of low sample concentration (10^{-5} M) in dichloromethane excited close to their maximum absorption wavelength relative to bithiophene ($\varphi_f = 0.013$). Phosphorescence measurements were done on a Varian Cary Eclipse (Dorval, QC, Canada) at 77 K in a 4:1 ethanol/methanol solvent. The same matrix was used for low temperature fluorescence measurements. The absolute energy difference (ΔE) was taken from the intercept of the normalized absorbance and fluorescence spectra for the corresponding compound. Meanwhile, the spectroscopic energy gap (E_g^{spec}) was calculated from the onset of absorbance.

Electrochemical methods

Cyclic voltammetry measurements were performed on a Bio Analytical Systems (West Lafayette, IN) EC Epsilon potentiostat. Compounds were dissolved in anhydrous and deaerated dichloromethane at 10^{-4} M with NBu_4PF_6 ranging between 10^{-2} and 10^{-3} M concentration to achieve conductive solutions. A platinum electrode was used as auxiliary and working electrodes, while a saturated Ag/AgCl (aq.) electrode was used as the reference electrode. To ensure consistent redox measurements between the various azomethines analysed, ferrocene was added at the end of each measurement and used as an internal reference.[31] The highest occupied molecular orbital (HOMO) values were calculated from the corresponding oxidation onset (E_{pa}^{onset}) according to $E_{pa}^{onset} + 4.4$ eV. Similarly, the lowest unoccupied molecular orbital (LUMO) values were calculated from the corresponding reduction onset (E_{pc}^{onset}) according to $E_{pc}^{onset} + 4.4$ eV.

Crystal structure determination

Diffraction data for **20** were collected on a Bruker FR591 diffractometer using graphite-monochromatized Cu K_α radiation with 1.54178 Å. The structures were solved by direct methods (SHELXS97). All nonhydrogen atoms were refined based on Fobs2 (SHELXS97), while hydrogen atoms were refined on calculated positions with fixed isotropic U, using riding model techniques.

Experimental for anodic coupled products

Single-sided indium tin oxide (ITO) coated plates were purchased from Delta Technologies (Loveland, CO, USA.) ($R_S = 5–10\ \Omega$). These were cut into rectangular shapes and were used as the working electrode. The substrates were used after cleaning with standard washing protocols with water, acetone and dichloromethane for 20 min followed by ultrasonication. The cross-coupled products were electrochemically produced by 50 repeated anodic scans ranging from 0 to 1.4 V at 100 mV/s in dichloromethane. Alternatively, the anodic coupling was done by applying an anodic potential 100 mV greater than the corresponding radical cation and held at the potential for 10 min in dichloromethane. In both cases, the cross-coupled products were physisorbed onto the ITO electrode. The transparent electrodes were removed from the reagent/electrolyte solution and rinsed thoroughly with dichloromethane to remove unreacted reagent and the supporting electrolyte. The electrode was then submerged in a dichloromethane solution of NBu_4PF_6 and a final potential of −100 mV was applied for 2 min to ensure the resulting products were in the neutral form.

Sufficient material of the anodically coupled product for standard characterization methods was obtained according to the experimental procedures described above with the exception of the working electrode. The button platinum working electrode was substituted with a large area platinum mesh gauze. Several milligrams of **19** were dissolved in anhydrous dichloromethane (75 mL) and a potential 100 mV greater than its first E_{pa} (i.e., 1.2 V) was applied for 20 min under a blanket of nitrogen. The resulting products were neutralized for 2 min by applying a potential of −100 mV. The solvent was removed under reduced pressure and the resulting product was dissolved in a mixture of ethyl acetate/diethyl ether (50:50) and the residual NBu_4PF_6 was removed by filtration.

Synthesis

The preparation of **1–2**, **13–14, 17** and **19–21** were done according to previously reported methods.[9,29,30]

*2-((1-Methyl-1H-pyrrol-2-yl)methyleneamino)thiophene-3-carbonitrile (**7**)*

3 (53 mg, 0.48 mmol) and **2** (60 mg, 0.48 mmol) were mixed in anhydrous isopropanol (20 mL) with a catalytic amount of trifluoroacetic acid (TFA) and then refluxed for 12 h. The reaction mixture was concentrated *in vacuo* and the crude mixture was purified by flash chromatography eluted with hexanes/ethyl acetate (90/10) up to hexanes/ethyl acetate (60/40) to afford the product as a yellow solid (30 mg, 60%). M.p.: 116–118 °C. ^{1}H-NMR (acetone-d_6): δ = 8.47 (s, 1H), 7.28 (d, 1H, ^3J = 5.7 Hz), 7.21 (d, 1H, ^3J = 5.7 Hz), 7.19 (dd, 1H, ^3J = 2.0 Hz and ^5J = 1.8 Hz), 6.95 (dd, 1H, ^3J = 4.0 Hz and ^5J = 1.7), 6.27 (dd, 1H, ^3J = 4.0 Hz and ^3J = 2.1 Hz), 4.12 (s, 3 Hz). ^{13}C-NMR (acetone-d_6): δ = 165.7, 151.6, 133.1, 129.5, 127.5, 122.9, 120.5, 115.1, 110.2, 104.0, 37.0. HRMS(+) calculated for $[C_{11}H_9N_3S + H]^+$: 216.05955 found 216.05889.

*2-((1H-Pyrrol-2-yl)methyleneamino)thiophene-3-carbonitrile (**8**)*

In a 50-mL round bottom flask, **2** (60 mg, 0.48 mmol) was dissolved in isopropanol (20 mL). To this was added, with vigorous stirring, **4** (46 mg, 0.48 mmol) and a catalytic amount of TFA followed by refluxing for 12 h. The title compound was isolated as a yellow powder (68%) after purification by flash chromatography (SiO_2) eluted with hexanes/ethyl acetate (90/10) up to hexanes/ethyl acetate (50/50). M.p.: 77–79 °C. ^{1}H-NMR (acetone-d_6): δ = 11.35 (s, NH), 8.45 (s, 1H), 7.29 (s, 1H, J = 1.8 Hz), 7.26 (d, 1H, J = 5.7 Hz), 7.19 (d, 1H, J = 5.7 Hz), 6.96 (t, 1H, J = 1.8 Hz), 6.37 (m, 1H, J = 1.8 Hz). ^{13}C-NMR (acetone-d_6): δ = 165.4, 151.2, 130.2, 127.8, 127.0, 120.6, 120.4, 115.1, 111.6, 103.5. HRMS(+) calculated for $[C_{10}H_7N_3S + H]^+$: 202.04334 found 202.04380.

*2-[(Thiophen-2-ylmethylene)-amino]-thiophene-3-carbonitrile (**9**)*

2 (50 mg, 0.40 mmol) and **5** (54 mg, 0.48 mmol) were mixed in anhydrous isopropanol (20 mL) with a catalytic amount of TFA and then refluxed for 20 h. The reaction mixture was concentrated and then purified by flash chromatography eluted with hexanes/ethyl acetate (90/10 v/v) up to hexanes/ethyl acetate (60/40 v/v) to afford the product as an orange solid (61 mg, 70 %). M.p.: 58–60 °C. ^{1}H-NMR (acetone-d_6): δ = 8.49 (s, 1H), 7.90 (d, 1H, J = 5.0 Hz), 7.82 (dd, 1H, ^3J = 3.7 Hz and 1.0 Hz), 7.42 (d, 1H, J = 5.7 Hz), 7.26 (d, 1H, J = 5.6 Hz), 7.26 (dd, 1H, J = 4.8 Hz and J = 3.5 Hz). ^{13}C-NMR (acetone-d_6): δ = 163.4, 155.4, 141.8, 136.2, 133.9, 129.0, 128.1, 122.5, 114.6, 105.8. HRMS(+) calculated for $[C_{10}H_6N_2S_2 + H]^+$: 219.00452, found: 219.00514.

*2-((Furan-2-yl)methyleneamino)thiophene-3-carbonitrile (**10**)*

6 (54 mg, 0.56 mmol) and **2** (70 mg, 0.56 mmol) were refluxed in anhydrous isopropanol (20 mL) in a 50-mL flask where the solution turned orange after 12 h of stirring under nitrogen. The solution was then concentrated under vacuum to near dryness. The crude product was loaded onto a silica column and eluted with hexanes/ethyl acetate (90/10) up to hexanes/ethyl acetate (75/25) to give the product as a yellow–orange solid (95 mg, 83 %). M.p.: 86–88 °C. ^{1}H-NMR (acetone-d_6): δ = 8.55 (s, 1H), 7.95 (d, 1H, J = 1.5 Hz), 7.45 (d, 1H, J = 5.7 Hz), 7.35 (d, 1H, J = 3.4 Hz), 7.30 (d, 1H, J = 5.7 Hz), 6.77 (dd, 1H, ^3J = 3.5 Hz and 1.7 Hz). ^{13}C-NMR (acetone-d_6): δ = 163.8, 151.7, 149.1, 148.4, 128.2, 122.6, 120.5, 114.6, 113.5, 106.0. HRMS(+) calculated for $[C_{10}H_6N_2OS + Na]^+$: 225.00930 found 225.00885.

*Diethyl 2-((1-methyl-1H-pyrrol-2-yl)methyleneamino)-5-aminothiophene-3,4-dicarboxylate (**11**)*

3 (32 mg, 0.29 mmol) and **1** (75 mg, 0.29 mmol) were mixed in anhydrous isopropanol (20 mL) with a catalytic amount of TFA and then refluxed for 12 h. The reaction mixture was concentrated and then purified by flash chromatography eluted with hexanes/ethyl acetate (50/50) to afford the product as a yellow solid (81 mg, 80%). M.p.: 130–132 °C. ^{1}H-NMR (acetone-d_6): δ = 7.94 (s, 1H), 7.35 (s, NH_2), 6.96 (dd, 1H, ^3J = 4.1 Hz and ^5J = 2.0 Hz), 6.64 (dd, 1H, ^3J = 3.9 Hz and ^5J = 1.8 Hz), 6.14 (dd, 1H, ^3J = 3.8 Hz and 2.5 Hz), 4.29 (q, 2H, J = 7.1 Hz), 4.21 (q, 2H, J = 7.1 Hz), 3.95 (s, 3H), 1.34 (t, 3H, J = 7.1 Hz), 1.28 (t, 3H, J = 7.1 Hz). ^{13}C-NMR (acetone-d_6): δ = 165.5, 164.4, 160.1, 144.3, 134.6, 130.2, 130.0, 128.0, 119.0, 109.1, 101.7, 61.0, 59.8, 36.7, 14.1, 14.1. HRMS(+) calculated for $[C_{16}H_{19}N_3O_4S + H]^+$: 350.11690 found 350.11781.

*Diethyl 2-((1H-pyrrol-2-yl)methyleneamino)-5-aminothiophene-3,4-dicarboxylate (**12**)*

4 (28 mg, 0.29 mmol) and **1** (75 mg, 0.29 mmol) were mixed in anhydrous isopropanol (20 mL) with a catalytic amount of TFA and followed by refluxing for 12 h. The reaction was

concentrated and then purified by flash chromatography eluted with hexanes/ether (50/50) up to diethyl ether (100%) to afford the product as an orange powder (74 mg, 76%). M.p.: 161–163 °C. ^{1}H-NMR (acetone-d_6): δ = 10.68 (s, NH), 7.92 (s, 1H), 7.34 (s, NH_2), 7.04 (dd, 1H, ^3J = 3.6 and ^5J = 2.4 Hz), 6.65 (dd, 1H, ^3J = 3.6 and ^5J = 2.2 Hz), 6.23 (dd, 1H, ^3J = 3.6 and 2.4 Hz). ^{13}C-NMR (acetone-d_6): δ = 165.3, 164.4, 160.0, 143.8, 134.5, 130.7, 127.6, 124.1, 116.3, 110.5, 101.8, 60.9, 59.8, 14.1, 14.0. HRMS(+) calculated for $[C_{15}H_{17}N_3O_4S + H]^+$: 336.10125 found 336.10208.

*Diethyl 2,5-bis((1-methyl-1H-pyrrol-2-yl)methyleneamino)thiophene-3,4-dicarboxylate (**15**)*

3 (200 mg, 1.83 mmol) and DABCO (200 mg, 1.83 mmol) were dissolved in anhydrous toluene (20 mL) at 0 °C followed by the slow addition of $TiCl_4$ (1.0 M, 1.83 mL, 1.83 mmol). **1** (90 mg, 0.35 mmol) was subsequently added and the reaction mixture was refluxed for 3–4 h. The solvent was evaporated and the product isolated as a red solid after purification by flash chromatography with 1% triethylamine in hexanes up to hexanes/ethyl acetate (50/50) (57 mg, 37%). M.p.: 134–136 °C. ^{1}H-NMR (acetone-d_6): δ = 8.33 (s, 2H), 7.11 (d, 2H, J = 2.0 Hz), 6.85 (dd, 2H, ^3J = 4.0 and ^5J = 1.8 Hz), 6.24 (dd, 2H, J = 4.0 Hz and 2.5 Hz), 4.29 (q, 4H, J = 7.1 Hz), 4.07 (s, 6H), 1.33 (t, 6H, J = 7.1 Hz). ^{13}C-NMR (acetone-d_6): δ = 163.5, 149.5, 149.3, 132.2, 129.9, 126.1, 121.8, 109.9, 60.9, 36.9, 14.1. HRMS(+) calculated for $[C_{22}H_{24}N_4O_4S + H]^+$: 441.15910 found 441.15811.

*Diethyl 2,5-bis((1H-pyrrol-2-yl)methyleneamino)thiophene-3,4-dicarboxylate (**16**)*

4 (173 mg, 1.74 mmol) and DABCO (195 mg, 1.74 mmol) were dissolved in anhydrous toluene (20 mL) at 0 °C followed by the slow addition of $TiCl_4$ (1.0 M, 1.74 mL, 1.74 mmol). **1** (90 mg, 0.35 mmol) was then added and the mixture was refluxed for 30 min. The title compound was isolated as a red solid (64 mg, 44%) after flash chromatography with hexanes/ether (34/66) with 1% triethylamine and up to diethyl ether (100%). M.p.: 185–187 °C. ^{1}H-NMR (acetone-d_6): δ = 10.98 (s, NH), 8.31 (s, 2H), 7.20 (d, 2H, J = 0.4 Hz), 6.87 (d, 2H, J = 1.2 and 2.0 Hz), 6.33 (d, 2H, J = 2.2 Hz), 4.26 (q, 4H, J = 7.1 Hz), 1.30 (t, 6H, J = 7.1 Hz). ^{13}C-NMR (acetone-d_6): δ = 163.4, 149.7, 149.4, 130.6, 126.0, 125.2, 119.0, 111.2, 60.9, 14.0. HRMS(+) calculated for $[C_{20}H_{20}N_4O_4S + H]^+$: 413.12780 found 413.12778.

*Diethyl 2,5-bis((furan-2-yl)methyleneamino)thiophene-3,4-dicarboxylate (**18**)*

In a 50-mL round bottom flask was added **6** (112 mg, 1.16 mmol) dissolved in anhydrous toluene (25 mL) to which was subsequently added DABCO (434 mg, 3.87 mmol) and $TiCl_4$ (1.0 M, 1.55 mL, 1.55 mmol) at 0 °C. **1** (100 mg, 0.39 mmol) was then added and the mixture was refluxed for 2 h after which the solvent was then evaporated. Purification by flash chromatography (SiO_2) with hexanes and increased up to hexanes/ethyl acetate (50/50) yielded the title product as a red solid (30 mg, 19%). M.p.: 145–147 °C. ^{1}H-NMR (acetone-d_6): δ = 8.40 (s, 2H), 7.91 (d, 2H, J = 1.2 Hz), 7.26 (d, 2H, J = 3.5 Hz), 6.74 (dd, 2H, J = 3.5 Hz and 1.8 Hz), 4.31 (q, 4H, J = 7.1 Hz), 1.34 (t, 6H, J = 7.1 Hz). ^{13}C-NMR (acetone-d_6): δ = 162.9, 152.2, 149.8, 147.9, 147.8, 127.5, 119.0, 113.4, 61.2, 14.0. HRMS(+) calculated for $[C_{20}H_{18}N_2O_6S + H]^+$: 415.09583 found 415.09530.

*N^1,N^4-Bis((1-methyl-1H-pyrrol-2-yl)methylene)benzene-1,4-diamine (**22**)*

In a 50-mL round bottom flask, 1,4-phenylenediamine (70 mg, 0.65 mmol) was dissolved in isopropanol (20 mL). To this was added **3** (139 µL, 1.36 mmol) and a catalytic amount of TFA with vigorous stirring followed by refluxing for 12 h. The title compound was isolated as a yellow solid (120 mg, 64%) by precipitation in ethyl acetate/hexanes (5/95). M.p.: 127–129 °C. ^{1}H-NMR (acetone-d_6): δ = 8.46 (s, 2H), 7.24 (s, 4H), 6.98 (t, 2H, J = 1.9 Hz), 6.73 (dd, 2H, ^3J = 3.8 Hz and ^5J =1.7 Hz), 6.18 (dd, 2H, J = 3.8 Hz and 2.6 Hz). ^{13}C-NMR (acetone-d_6): δ = 150.4, 150.3, 130.9, 129.6, 121.9, 118.6, 108.9, 36.4. HRMS(+) calculated for $[C_{18}H_{18}N_4 + H]^+$: 291.16042 found 291.16030.

*N^1,N^4-Bis((1H-pyrrol-2-yl)methylene)benzene-1,4-diamine (**23**)*

In a 50-mL round bottom flask, 1,4-phenylenediamine (70 mg, 0.65 mmol) was dissolved in isopropanol (20 mL). To this was added **4** (129 mg, 1.36 mmol) with vigorous stirring along with a catalytic amount of TFA followed by refluxing for 12 h. The title compound was isolated as a yellow powder (147 mg, 86%) by precipitation in ethyl acetate/hexanes (5/95). M.p.: 205–207 °C. ^{1}H-NMR (acetone-d_6): δ = 10.93 (s, NH), 8.40 (s, 2H), 7.23 (s, 4H), 7.10 (s, 2H), 6.71 (dd, 2H, ^3J = 3.5 Hz and ^5J =1.3 Hz), 6.27 (dd, 2H, J = 3.4 Hz and 2.7 Hz). ^{13}C-NMR (acetone-d_6): δ = 150.0, 149.2, 131.7, 123.5, 122.0, 116.3, 110.1. HRMS(+) calculated for $[C_{16}H_{14}N_4 + H]^+$: 263.12912 found 263.12930.

*N^1,N^4-Bis((thiophen-2-yl)methylene)benzene-1,4-diamine (**24**)*

In a 50-mL round bottom flask, 1,4-phenylenediamine (70 mg, 0.65 mmol) was dissolved in isopropanol (20 mL). To this was added **5** (124 µL, 1.36 mmol) with vigorous stirring and a catalytic amount of TFA followed by refluxing for 12 h. The title compound was isolated as a yellow solid (163 mg, 85%) by precipitation in ethyl acetate/hexanes (5/95). M.p.: 171–173 °C. ^{1}H-NMR (acetone-d_6): δ = 8.84 (s, 2H), 7.74 (d, 2H, J = 5.0 Hz), 7.67 (d, 2H, J = 3.5 Hz), 7.35 (s, 4H), 7.23 (dd, 2H, J = 4.5 Hz and 3.8 Hz). ^{13}C-NMR (acetone-d_6): δ = 153.0, 149.8, 143.7, 133.2, 130.8, 128.3, 122.4. HRMS(+) calculated for $[C_{16}H_{12}N_2S_2 + H]^+$: 297.05147 found 297.05132.

*N^1,N^4-Bis((furan-2-yl)methylene)benzene-1,4-diamine (**25**)*

In a 50-mL round bottom flask, 1,4-phenylenediamine (70 mg, 0.65 mmol) was dissolved in isopropanol (20 mL). To this, was added **6** (113 µL, 1.36 mmol) with vigorous stirring and a catalytic amount of TFA followed by refluxing for 12 h. The title compound was isolated as a yellow powder (115 mg, 67%) by precipitation in ethyl acetate/hexanes (5/95). M.p.: 144–146 °C. ^{1}H-NMR (acetone-d_6): δ = 8.49 (s, 2H), 7.83 (d, 2H, J = 1.4 Hz), 7.34 (s, 2H), 7.12 (d, 2H, J = 3.4 Hz), 6.69 (dd, 2H, J = 3.4 Hz and 1.8 Hz). ^{13}C-NMR (acetone-d_6): δ = 153.8, 150.7, 148.2, 146.8, 122.8, 116.5, 113.1. HRMS(+) calculated for $[C_{16}H_{12}N_2O_2 + H]^+$: 265.09715 found 265.09747.

RESULTS AND DISCUSSION

Spectroscopy

The series of compounds reported in Chart 1 were prepared to investigate the effect of the heterocycles in addition to the degree of conjugation on the electrochemical and photophysical

properties. In particular, the fluorescence, fluorescence quantum yields and phosphorescence of the various azomethines were investigated. Upon comparing spectroscopic properties of the similar heterocyclic compounds for example, **7**, **11** and **15** in Table 1 and Fig. 1, the effect of the degree of conjugation on the spectroscopic properties can be elucidated. In all cases, both the absorbance and fluorescence maxima were bathochromically shifted by about 70 nm upon progressing from the dyads to the triads. Meanwhile, the homoaryl derivatives **22–25** exhibited absorbance and fluorescence maxima comparable to their corresponding dyads. This is in contrast to the homoaryl benchmark **26**, whose absorbance and fluorescence maxima that are hypsochromically shifted relative to the triads. The spectroscopic data confirm that extended degrees of conjugation are possible with the heterocyclic derivatives relative to their homoaryl azomethines.

Although an unsubstituted amino derivative of **1** would be advantageous for direct comparison of the properties with **26**, this is not possible owing to the instability of both such a precursor and its corresponding azomethines. **1** was used in lieu of preparing the targeted compounds because both **1** and its azomethine derivatives are stable under ambient conditions. Although an ester derivative of **2** is preferred for direct property comparison for compounds prepared from **1** and **2**, the ester analogues of **7–10** were unstable, precluding their characterization. Despite this, the azomethines derived from **1** and **2** can be compared owing to the similar electron withdrawing effect of the cyano and ester groups.[32,33] Moreover, given that **1** and **2** were used for preparing all the heterocyclic azomethines, the effect of their electron withdrawing group on the observed properties is consistent for all the azomethine derivatives.

The general trend of the various heterocycles' impact on the spectroscopic properties is represented in Fig. 1. It is evident that the absorbance is bathochromically shifted by about 30 nm for each heterocycle upon progressing in the order of furan < thiophene < pyrrole < methyl pyrrole for the symmetric azomethines. The same trend was observed for all the azomethines studied and is consistent with the increasing electron richness of the heterocycle.[38] In the case of the unsymmetric azomethines, the spectroscopic properties resemble those of the corresponding symmetric azomethines with the greatest electron-rich heterocycle.

Although the azomethine bond is electron withdrawing, its electronic effect is insufficient to offset any gain achieved by increasing the degree of conjugation. This is corroborated by the spectral bathochromic shifts observed for **15–18** relative to their dyad analogues **7–10**. The limited spectroscopic property perturbation from the electronic groups is further evidenced from the dyads **7–14**. This is apparent from the absorption spectra of **11–14** that are shifted by only 10 nm relative to **7–10**, while the fluorescence spectra are relatively similar, despite the strong electron donating group in the terminal position of **11–14**. The terminal amine's donating effect is most likely further offset by the adjacent withdrawing ester. The collective spectroscopic data confirm that the spectroscopic properties are governed more by the degree of conjugation than the electronic groups along the conjugated framework, which affect predominately the redox potentials (*vide infra*). Direct property comparison of the 3-monocyano substituted azomethines (**7–10**) to their 3,4-disubstituted counterparts (**11–18**) is therefore possible because the additional cyano group is not expected to significantly affect the spectroscopic properties. The spectroscopic data further imply that the homoaryl **26** is a suitable reference for benchmarking the spectroscopic properties. Comparing the data of the various compounds, it is evident that the spectroscopic properties can discretely be tailored as a function of structure and heterocycle. The significant bathochromic shifts observed for the heterocyclic azomethines relative to the homoaryl analogues imply that the heterocyclic derivatives have enhanced delocalization. This is most likely due in part to the high degree of coplanarity (*vide infra*) of the heterocyclic azomethines combined with the electronic effects of the π-rich heterocycles. Also, the steady-state spectroscopic data suggest that the degree of conjugation for the homoaryl derivatives **22–25** is confined to the heterocycle–azomethine moiety and that delocalization across the entire molecule is reduced. This is in part based on their hyposchromic shifts relative to their respective analogues **15–18**.

All the compounds studied exhibited weak fluorescence quantum yields (Φ_f) on the order of $< 10^{-3}$. This is in contrast to their vinylene analogues that fluoresced with Φ_f ranging between 0.68 and 0.99.[39,40] Although many assumptions are made for deriving quantum yields relative to standards such as bithiophene ($\Phi_f = 0.013$), the fluorescence for all the compounds is nonetheless extremely low. We verified the accuracy of the fluorescence measurements using an integrating sphere. This provides absolute fluorescence yields regardless of the excitation and emission wavelengths and emission yields.[41] The fluorescence yields for the azomethines were all below the detection limit ($\Phi_f < 0.01$), confirming the quenched fluorescence regardless of the degree of conjugation and type of heterocycle.

Low temperature fluorescence measurements were subsequently undertaken to gain insight into the origins of the fluorescence quenching and deactivation modes of the azomethines. At 77 K, internal conversion deactivation modes by either simple bond rotation or intramolecular processes requiring geometric alignment and bond rotations are suppressed. Increased fluorescence should therefore be observed if nonradiative internal conversion deactivation by either of these rotation modes is an efficient deactivation manifold. Homogeneous glass matrices suitable for low temperature measurements were done with a 4:1 ethanol/methanol matrix.

As seen in Table 1, the low temperature fluorescence is several orders of magnitude greater than that at room temperature. The measured values suggest that the fluorescence can be restored to near quantitative values at low temperature. The azomethines therefore have temperature sensor-like properties such that the fluorescence can be *turned-on* and *turned-off* with temperature. Although the temperature dependent fluorescence confirms that the singlet excited state of the azomethines is deactivated by internal conversion, the quantum yield of this process cannot be accurately measured. This is a result of the large error associated in comparing the intense fluorescence signal at 77 K to the extremely noisy and weak room temperature signal (inset Fig. 1). The temperature-dependent fluorescence nonetheless confirms that the azomethine fluorescence is temperature dependent. It further confirms that deactivation by internal conversion involving bond rotation/alignment is a major deactivation mode of azomethine singlet excited state deactivation. Meanwhile, deactivation of the singlet manifold is consistent for all the azomethines and is independent of the type of heterocycle and degree of conjugation. It is noteworthy that weak fluorescence was observed regardless of solvent polarity and proticity

Table 1. Spectroscopic[a] and electrochemical[b] data for the various symmetric and unsymmetric[c] azomethines

	Compound	Abs (nm)[d]	Fluo (nm)[e]	Φ_{fl}[f] ($\Phi_{77\ K}$)[g]	ΔE (eV)[h]	E_g^{spec} (eV)[i]	E_{pa} (V)	E_{pc} (V)	E_g (eV)[j]	HOMO (−eV)[k]	LUMO (−eV)[k]	$E_{pa}^{(ITO)}$ (V)[l]	$E_{pc}^{(ITO)}$ (V)[l]	abs^{ITO} (nm)[l]
	1	305	335	2.5×10^{-3} (8.9×10^{-3})	3.7	3.0	0.6	—	—	4.9	1.2	—	—	—
	2	279	304	3×10^{-6} (7.7×10^{-6})	4.2	3.9	1.3	—	—	5.6	1.5	—	—	—
Dyads	7	382	473	9.4×10^{-5} (0.76)	2.9	2.7	1.4	−1.6	2.9	5.7	2.8	1.3	−1.1	439
	8	380	472	1.1×10^{-4} (0.42)	3.0	2.7	1.4	−1.6	2.9	5.7	2.8	1.3	−1.1	433
	9	370	439	3.9×10^{-3} (0.79)	3.2	2.7	1.7	−1.4	3.0	6.0	3.0	1.3	−1.2	433
	10	363	429	2.3×10^{-4} (0.56)	3.1	2.8	1.7	−1.4	3.0	6.0	3.0	1.4	−1.1	412
	11	390	472	4.3×10^{-4} (0.59)	2.9	2.7	0.8	−1.9	2.6	5.1	2.5	0.6	−1.3	424
	12	391	474	2.6×10^{-4} (0.48)	2.9	2.7	0.8	−1.9	2.6	5.1	2.5	0.6	−1.4	430
	13	400	480	2.9×10^{-3} (0.97)	2.9	2.6	1.0	−1.4	2.3	5.3	3.0	0.7	−1.2	434
	14	390	469	7.7×10^{-4} (0.88)	2.9	2.7	1.0	−1.3	2.2	5.3	3.1	0.7	−1.4	431
Triads	15	457	538	5.1×10^{-3} (0.82)	2.5	2.3	0.8	−1.4	2.1	5.1	3.0	0.8	−1.1	486
	16	452	504	2.5×10^{-3} (0.88)	2.6	2.3	1.0	−1.4	2.3	5.3	3.0	0.8	−1.2	483
	17	440	534	2.8×10^{-3} (0.74)	2.6	2.3	0.9	−1.3	2.1	5.2	3.1	0.7		485
	18	430	494	9.6×10^{-4} (0.81)	2.8	2.4	1.0	−1.2	2.1	5.3	3.2	0.8	−1.3	480
	19	457	531	3.8×10^{-4} (0.39)	2.4	2.2	1.0	−1.3	2.2	5.3	3.1	0.7	−1.2	483
	20	452	531	1.2×10^{-3} (0.43)	2.5	2.3	1.1	−1.3	2.3	5.4	3.1	1.0	−1.1	477
	21	420	519	6.5×10^{-4} (0.21)	2.6	2.3	1.1	−1.2	2.2	5.4	3.2	0.8	−1.3	455
Analogues	22	367	419	1.2×10^{-3} (0.71)	3.2	2.8	1.0	−2.2	3.1	5.3	2.2	0.8	−1.3	404
	23	365	404	3.3×10^{-3} (0.69)	3.1	2.7	1.0	−2.2	3.1	5.3	2.2	0.8	−1.2	397
	24	366	416	3.7×10^{-4} (0.63)	3.1	2.9	1.4	−1.8	3.1	5.7	2.6	1.3	−1.2	420
	25	360	422	4.6×10^{-4} (0.59)	3.2	2.9	1.3	−1.8	3.0	5.6	2.6	1.0	−1.4	448
	26[m]	354	410	0.68–0.99	—	2.7	—	—	—	—	—	—	—	—

[a]In anhydrous acetonitrile.
[b]Values reported against Ag/AgCl (sat'd) in CH_2Cl_2.
[c]Literature values.[30]
[d]Absorbance maximum.
[e]Emission maximum.
[f]Fluorescence quantum yields at $\lambda_{ex} = 303$ nm, relative to bithiophene.[34]
[g]Values in parentheses are absolute fluorescence quantum yields at 77 K relative to room temperature.
[h]Absolute HOMO–LUMO spectral difference.
[i]Spectroscopic energy gap.
[j]Electrochemical energy gap.
[k]HOMO and LUMO values were determined from the oxidation and reduction onsets, respectively, relative to vacuum.
[l]Data for anodically coupled products immobilized on ITO electrodes.
[m]Literature values.[35–37]

implying that simple polar effects and perturbation of the singlet–triplet manifolds are not the reason for the quenched fluorescence. It is further noteworthy that the emission wavelength does not shift with temperature (inset Fig. 1). This implies that the compounds adopt a similar extended degree of conjugation arrangement both in the solid matrix and at room temperature. The temperature induced fluorescence *turn-on* makes the azomethines interesting fluorimetric temperature sensors.

Laser flash photolysis (LFP) was used to further investigate the excited state deactivation modes of the azomethines. Short-lived transients on the order of μs can be spectroscopically detected and assigned by this time resolved method. No transient was detected for any of the azomethines, implying that intramolecular deactivation involving either radical or radical ion transients does not occur. Although no signal was measured by LFP, triplet formation by intersystem crossing (ISC) cannot be unequivocally dismissed. This is because the shortest transient

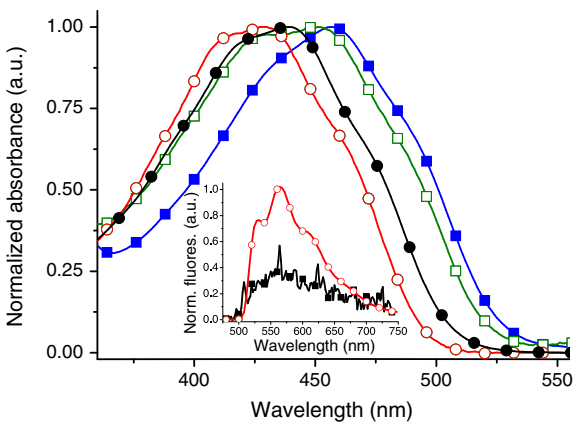

Figure 1. Effect of different heterocycles on the absorbance spectra: **15** (■), **16** (□), **17** (●), **18** (○). Inset: fluorescence of **20** at room temperature magnified 400 times (■) and 77 K (○)

lifetime detectable by the system is ≈100 ns and triplet quenching by intramolecular energy transfer would occur on a shorter timescale. Phosphorescence measurements were subsequently done in a glass matrix at 77 K. At this low temperature, collisional deactivation processes that would otherwise thermally deactivate the triplet are eliminated. Weak phosphorescence should subsequently be seen if the triplet state is formed. Even though phosphorescence (see Supporting Information) was observed for all the azomethines studied, only qualitative information regarding the triplet state can be obtained given that $\Phi_{phos} < \Phi_{ISC}$. Azomethine phosphorescence confirms that the triplet is produced at 77 K and that it is efficiently deactivated at room temperature.

In light of the high fluorescence yields measured at low temperatures, deactivation by ISC is not a major deactivation mode. The collective steady-state and time-resolved spectroscopic data confirm that the suppressed fluorescence is predominately a result of deactivation of the singlet excited state by internal conversion involving bond rotation. The fluorescence can therefore be restored at low temperatures by suppressing these energy wasting modes. Meanwhile, the steady-state spectroscopic data confirm that both the absorbance and fluorescence are contingent not only on the nature of the heterocycle, but also on the number of azomethine bonds. Also, significant absorbance and fluorescence bathochromic shifts are possible with the heterocyclic azomethines relative to their homoaryl containing counterparts. It is evident from the data that the color and fluorescence emission can be discretely tuned to nearly any wavelength, contingent of heterocycle, degree of conjugation and electronic effects. Heterocyclic azomethines therefore exhibit enhanced functional materials-like properties relative to their homoaryl analogues and similar properties to those of their vinylene counterparts.

Crystallographic data

Single crystal X-ray diffraction analysis of **20** was investigated to determine the twisting between the aryl–azomethine planes. The X-ray crystallography data shown in Fig. 2 confirm that **20** is unsymmetric and that it consists of a central thiophene sandwiched between a furan and pyrrole. The figure also shows that the heterocycles adopt an antiparallel arrangement. It is further evident that the two connecting azomethine bonds both adopt the *E* isomer and that the compound is linear. Most importantly, the mean plane angles between the terminal heterocycles and the central thiophene are about 18°.

The crystallographic data for **11–21**[6,30,42–46] were compiled to examine the effect of the various heterocycles on the molecular arrangement and for further understanding the spectroscopic data. The data are collectively summarized in Table 2. It can be seen that the mean plane angles between the terminal heterocycles and the central thiophene range between 2.5–34°. This is in contrast to their homoaryl derivative **23** whose analogous mean planes are twisted between 32.9 and 56.4°.[47] The consistent large aryl–azomethine twisting angle of the homoaryl derivatives imply a reduced degree of conjugation and reduced delocalization of the phenylene azomethines relative to their heterocycle counterparts. Meanwhile, the antiparallel and coplanar arrangements of **11–21** contribute to the enhanced degree of conjugation of the heterocyclic derivatives. The azomethine and azomethine–aryl bonds were found to be shorter than the corresponding CH–aryl bonds. This suggests an increased degree of conjugation of the azomethines relative to their homologues, resulting in delocalization of the electron-rich heterocycles across the entire molecule. This is responsible for the strong visible absorbance and emission properties of the heterocyclic azomethines. Also, given that no temperature-dependent emission shifts were observed, the configuration observed in the crystal state is most likely comparable to that adopted in solution.

According to Fig. 3, the crystal packing shows several interactions between the pyrrole–furan moieties. These are consistent with donor–acceptor type interactions between the two heterocycles. These interactions can be assumed from the centroid-to-centroid distance (3.808 Å) and the interatom distances (3.3–3.6 Å) that are below the sum of the van der Waals radii (3.4–3.5 Å). The donor–acceptor interactions lead to regio-regular crystal packing involving alternating pyrrole–furan repeating motifs. Although hydrogen bonding is nonexistent

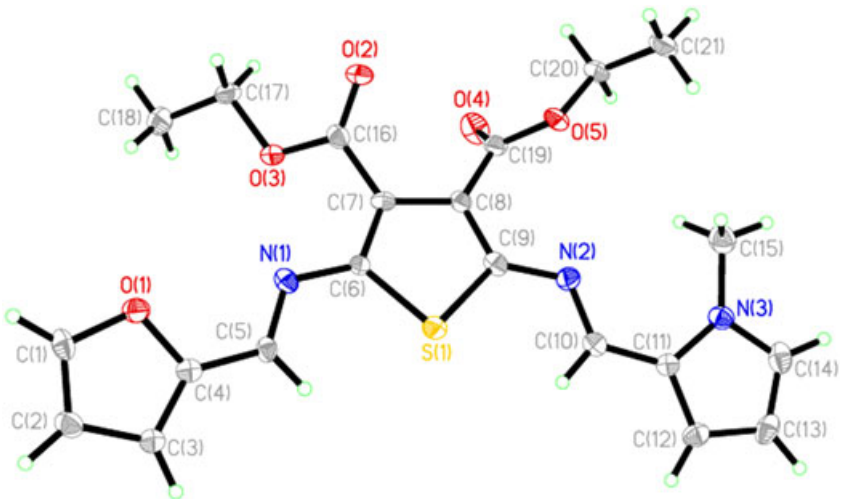

Figure 2. ORTEP representation of **20** with the ellipsoids drawn at 30% probability

Table 2. Selected crystallographic data of **11–21**

	11	12	13	14	15[a]		16		17		18[a]		19		20		21[a]	
	Side N	Side N	Side S	Side O	Side N1	Side N2	Side N1	Side N2	Side S1	Side S2	Side O1	Side O2	Side N	side S	side N	side O	side S	side O
Plane angle (°)[b]	17.06(4)	10.2(1)	9.0(1)	2.51(4)	10.8(2)	19.5(2)	18.90(5)	10.31(4)	9.04(4)	25.07(6)	7.1(2)	30.8(2)	3.5(2)	3.5(1)	18.0(2)	18.8(2)	33.6(4)	7.9(5)
–C = N– (Å)	1.292(2)	1.275(2)	1.283(3)	1.289(2)	1.288(4)	1.286(4)	1.292(2)	1.384(2)	1.277(3)	1.286(3)	1.284(4)	1.285(4)	1.30(2)	1.279(9)	1.287(5)	1.287(4)	1.286(4)	1.286(4)
=N–Aryl– (Å)	1.372(2)	1.376(2)	1.381(3)	1.382(2)	1.378(4)	1.374(4)	1.383(2)	1.297(2)	1.381(3)	1.393(3)	1.377(4)	1.379(4)	1.373(2)	1.377(2)	1.374(5)	1.374(5)	1.381(4)	1.385(4)
=CH–Aryl– (Å)	1.424(2)	1.433(2)	1.426(3)	1.420(2)	1.425(4)	1.428(4)	1.441(2)	1.435(2)	1.443(3)	1.435(3)	1.427(4)	1.432(4)	1.434(9)	1.436(9)	1.419(5)	1.419(5)	1.435(4)	1.418(4)

[a]The average of the two molecules present per unit cell was taken.
[b]Refers to the mean plane angle between the central thiophene and the terminal heterocycles.

for **20**, unlike other azomethines such as **11–14**, the heterocyclic donor–acceptor interactions are sufficiently strong as evidenced by the fact that X-ray quality crystals of this unsymmetric compound could be easily obtained. Nonetheless, the collective coplanarity of the aryl–azomethine segments and the short bond distances are responsible for the significantly different spectroscopic properties between the homo- and heterocyclic azomethines.

Electrochemistry

Cyclic voltammetry was undertaken to further investigate the contribution of the various heterocycles and degree of conjugation on the oxidation (E_{pa}) and reduction potentials (E_{pc}). A typical voltammogram is seen in Fig. 4. The effect of the different heterocycles is evident from the E_{pa} for **7–10**. As seen in Table 1, the E_{pa} for the furan and thiophene derivatives are between 100 and 300 mV more positive than their corresponding pyrrole analogues. Conversely, the E_{pc} of the furan and thiophene derivatives are less positive than their pyrrole counterparts. These trends are independent of the degree of conjugation and are consistent with the π-richness of the heterocycle.[38]

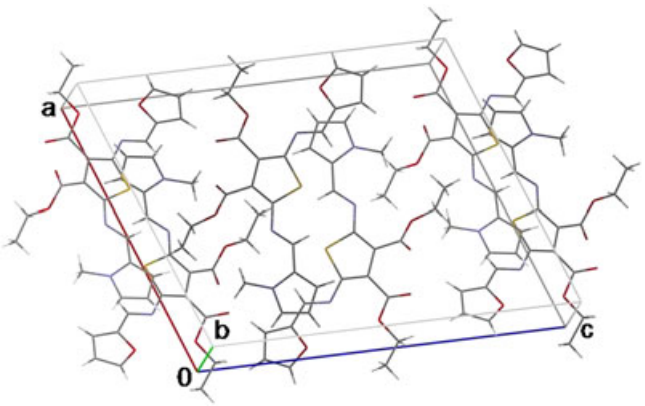

Figure 3. Extended view along the *ac* axis of the crystal lattice of **20**

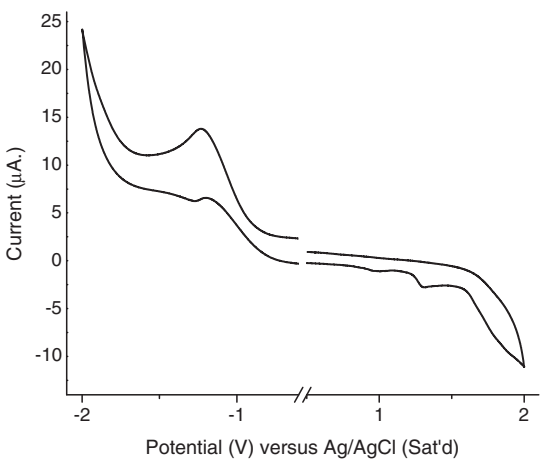

Figure 4. Cyclic voltammogram of **18** measured in anhydrous and deaerated dichloromethane at a scan rate of 100 mV/s

The electronic effect on the oxidation potential is evident upon comparing the E_{pa} of **11–14** to their corresponding dyads. The electron donating terminal amine reduces the E_{pa} by about 600 mV. Meanwhile, the same reduction in E_{pa} occurs with the additional azomethine for the triads relative to the corresponding dyads. The reduced E_{pa} is a result of the increased degree of conjugation and confirms the extended delocalization of the azomethines. The higher E_{pa} and energy gap (E_g) of the homoaryl derivatives (**22–25**) relative to their all-heterocyclic counterparts corroborate the limited degree of conjugation that was spectroscopically observed. The collective electrochemical data confirm that both the anodic and cathodic potentials can be tailored by incorporating different heterocycles into the azomethines and via the number of azomethine bonds.

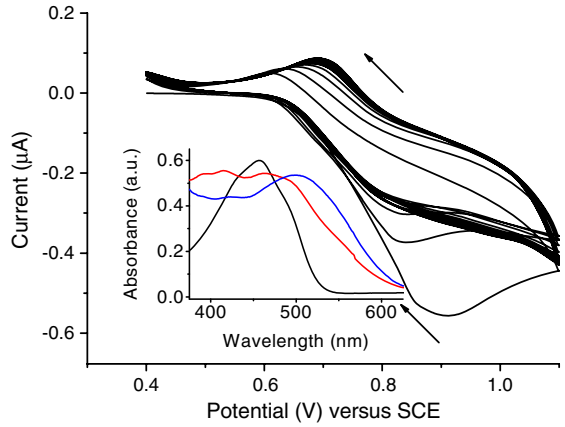

Figure 5. Anodic coupling of **15** at 100 mV/s in dichloromethane. Inset: absorbance of **15** deposited on ITO an electrode after applying E_{pa} = 1 V for 0 (black), 1 (red) and 5 min (blue)

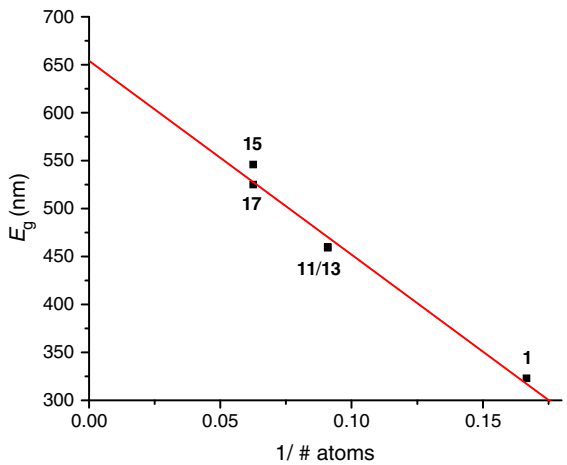

Figure 6. Evolution of spectroscopic E_g as a function of the number of atoms along the conjugated framework for the methyl-pyrrole and thiophene containing dyads and triads

Anodic coupling

As seen in Fig. 5, both the oxidation and reduction processes of **18** are irreversible. This behaviour is consistent for all the azomethines reported in Chart 1. It can be argued that the irreversible processes are a result of azomethine decomposition and reduction of the heteroconjugated bond. The latter can be dismissed because the cathodic process was found to be a one-electron transfer, determined relative to ferrocene. Conversely, azomethine reduction is a two-electron process. The anodic process is similarly a one-electron transfer process resulting in the radical cation. The irreversible oxidation is a result of radical cation cross-coupling according to standard means.[48,49] This was previously determined with terminally substituted derivatives such as **27** that were found to yield persistent radical cations.[6,7,50,51]

In light of the unsubstituted 2,2′-terminal positions of the heterocyclic azomethines, we investigated whether the radical cation could undergo standard cross-coupling to afford coupled products with increased degrees of conjugation. This was done both by cyclic oxidation scans and chronometrically by applying a potential slightly more positive than the E_{pa} of the azomethine of study. ITO-coated glass electrodes were used for spectroscopically and electrochemically characterizing the anodically coupled products physisorbed to the transparent electrode. A typical voltammogram of the anodic coupling is represented in Fig. 5 for **15**. The anodic wave shifts to less positive potentials with cycling between 1.1 and 0.4 V concomitant with a shift of the cathodic wave to more positive potentials. The former implies that the anodically coupled product is more conjugated than its corresponding monomer. Moreover, the resulting product physisorbed to the electrode exhibited a one-electron reversible oxidation. The increased degree of conjugation is further confirmed by a 30-nm bathochromic shift in the absorbance relative to the original **15**. To ensure that the measured properties were that of the neutral product and not

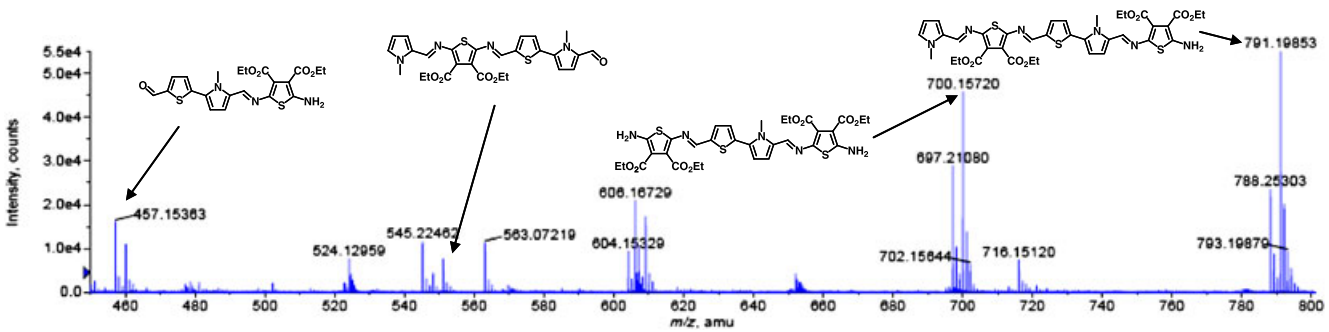

Figure 7. Mass spectrum of **P19** in positive ESI mode

its corresponding oxidized intermediate, a potential of 0 V was applied for 2 min prior to measuring the E_{pa} of the coupled products.

Less positive E_{pa} and bathochromic absorbance shifts were observed for the anodically coupled products of all the azomethines. Given that the anodic coupling of **11–14** can only yield dimers, their similar absorbance shifts to the other anodically coupled products in Chart 1 suggest that the anodically coupled products **P15–P25** are low molecular weight oligomers. This was spectroscopically investigated with a calibration curve of absorbance as a function of the reciprocal number of atoms along the conjugated framework (Fig. 6). The estimated degree of oligomerization determined by this method for **15** is two. Both the oxidation and absorbance shifts nonetheless provide the first reported evidence for anodically coupled products where increased degrees of conjugation relative to their corresponding monomers are formed.

Absolute evidence for coupled product formation was further sought to corroborate the qualitative spectroscopic data obtained from the anodically coupled products deposited on the ITO electrodes. **19** was therefore anodically coupled using a large surface area platinum mesh gauze for obtaining sufficient material for standard characterization. However, only minute amounts of soluble product for mass spectrometry analyses were isolated. The resulting Electrospray Ionisation (ESI) mass spectrum is shown in Fig. 7. The major molecular ion peaks ($m/z = 791$ and 700) confirm that anodically coupled products are formed. The weaker molecular ion peaks ($m/z = 457$ and 545) suggest some azomethine hydrolysis, which most likely occurs during analysis/sample preparation. Although higher order oligomers or polymers cannot be confirmed because of their reduced solubility, the mass spectrometry (MS) data nevertheless provide information relating to the lower molecular weight limit of the coupled products that are produced. It is noteworthy that azomethine anodic product coupling has not previously been confirmed. The collective MS and spectroscopic data provide unprecedented supporting evidence that anodic coupling occurs and that products with increased degree of conjugations relative to **19** are formed. The data further suggest that anodically produced polyazomethine is possible, providing its oligomeric precursors do not precipitate during anodic coupling. This would be possible with 3,4-dialkylated monomer derivatives of **15–21**.

CONCLUSION

Conjugated azomethines consisting uniquely of heterocycles were prepared. It was found that both the spectroscopic and electrochemical properties of azomethines were contingent on the heterocycles and number of azomethine bonds. Although such behaviour is expected from chemical intuition, the first examples unequivocally confirming these properties with azomethines containing exclusively heterocycles were presented. It was also found that the suppressed fluorescence of azomethines could be restored at low temperatures. This opens the possibility of using conjugated azomethines as sensors. Meanwhile, anodic coupling was demonstrated with products of increased degree of conjugation being formed. The collective observed spectroscopic and electrochemical data confirm that azomethine property tailoring is possible by modifying the degree of conjugation, number of azomethines and type of heterocycle. The azomethines investigated illustrate that heterocyclic azomethines are robust and that functional materials-like properties are possible. Future generation of materials for a given application can therefore be prepared with the knowledge gained from the discovered fluorescence *turn-on* and *turn-off*, oxidation potentials and property tailoring contingent on structure.

Acknowledgements

Natural Sciences and Engineering Council Canada (NSERC) Canada is thanked for Discover and Research Tools and Instruments grants allowing this work to be performed in addition to Canada Foundation for Innovation for additional equipment funding. S.D. also thanks NSERC for a graduate scholarship. W.G.S. also acknowledges both the Alexander von Humboldt Foundation and the Royal Society of Chemistry for a JWT Jones Travelling fellowship, allowing the completion of this manuscript.

REFERENCES

[1] H. Ma, H.-L. Yip, F. Huang, A. K. Y. Jen, *Adv. Funct. Mater.* **2010**, *20*, 1371.
[2] K. T. Kamtekar, A. P. Monkman, M. R. Bryce, *Adv. Mater.* **2010**, *22*, 572.
[3] J. Roncali, *Acc. Chem. Res.* **2009**, *42*, 1719.
[4] P. M. Beaujuge, J. R. Reynolds, *Chem. Rev.* **2010**, *110*, 268.
[5] J. Mei, K. R. Graham, R. Stalder, J. R. Reynolds, *Org. Lett.* **2010**, *12*, 660.
[6] S. Dufresne, A. Bolduc, W. G. Skene, *J. Mater. Chem.* **2010**, *20*, 4861.
[7] A. Bolduc, S. Dufresne, W. G. Skene, *J. Mater. Chem.* **2010**, *20*, 4820.
[8] M. Sun, C. Zhong, F. Li, Y. Cao, Q. Pei, *Macromolecules* **2010**, *43*, 1714.
[9] M. Bourgeaux, S. A. Perez Guarin, W. G. Skene, *J. Mater. Chem.* **2007**, *17*, 972.
[10] C.-J. Yang, S. A. Jenekhe, *Chem. Mater.* **1991**, *3*, 878.
[11] A. Iwan, P. Bilski, H. Janeczek, B. Jarzabek, M. Domanski, P. Rannou, A. Sikora, D. Pociecha, B. Kaczmarczyk, *J. Molecul. Struc.* **2010**, *963*, 175.
[12] S. Dufresne, S. A. P. Guarìn, A. Bolduc, A. N. Bourque, W. G. Skene, *Photochem. Photobiol. Sci.* **2009**, *8*, 796.
[13] S. Dufresne, L. Callaghan, W. G. Skene, *J. Phys. Chem. B* **2009**, *13*, 15541.
[14] A. N. Bourque, S. Dufresne, W. G. Skene, *J. Phys. Chem. C* **2009**, *113*, 19677.
[15] K. Suematsu, K. Nakamura, J. Takeda, *Colloid. Polym. Sci.* **1983**, *261*, 493.
[16] A. Rembaum, in: *United States Patent Offce*, California Institute of Technology, United States, **1981**, 6.
[17] D. Pont, E.I. Du Pont De Nemours and Company, Great Britain, **1967**, 8.
[18] D. Sek, B. Jarzabek, E. Grabiec, B. Kaczmarczyk, H. Janeczek, A. Sikora, A. Hreniak, M. Palewicz, M. Lapkowski, K. Karon, A. Iwan, *Synth. Met.* **2010**, *160*, 2065.
[19] D. Sek, A. Iwan, B. Kaczmarczyk, B. Jarzabek, J. Kasperczyk, H. Bednarski, *High Perf. Polym.* **2007**, *19*, 401.
[20] F.-C. Tsai, C.-C. Chang, C.-L. Liu, W.-C. Chen, S. A. Jenekhe, *Macromolecules* **2005**, *38*, 1958.
[21] C.-P. Chang, C.-C. Wang, C.-Y. Chao, M.-S. Lin, *J. Polym. Res.* **2005**, *12*, 1.
[22] S. Destri, M. Pasini, C. Pelizzi, W. Porzio, G. Predieri, C. Vignali, *Macromolecules* **1998**, *32*, 353.
[23] A. G. El-Shekeil, F. A. Al-Yusufy, S. Saknidy, *Polym. Int.* **1997**, *53*, 777.
[24] C. Wang, S. Shieh, E. LeGoff, M. G. Kanatzidis, *Macromolecules* **1996**, *29*, 3147.
[25] C.-J. Yang, S. A. Jenekhe, *Macromolecules* **1995**, *28*, 1180.
[26] C. Amari, C. Pelizzi, G. Predieri, S. Destri, W. Porzio, *Synth. Met.* **1995**, *72*, 7.

[27] S. B. Park, H. Kim, W. C. Zin, J. C. Jung, *Macromolecules* **1993**, *26*, 1627.
[28] S. Dufresne, I. U. Roche, T. Skalski, W. G. Skene, *J. Phys. Chem.* **2010**, *114*, 13106.
[29] S. Dufresne, M. Bourgeaux, W. G. Skene, *J. Mater. Chem.* **2007**, *17*, 1166.
[30] S. Dufresne, W. G. Skene, *J. Org. Chem.* **2008**, *73*, 3859.
[31] N. G. Connelly, W. E. Geiger, *Chem. Rev.* **1996**, *96*, 877.
[32] G. Hallas, A. D. Towns, *Dyes Pigm.* **1997**, *33*, 205.
[33] Y. Ooyama, G. Ito, K. Kushimoto, K. Komaguchi, I. Imae, Y. Harima, *Org. Biomol. Chem.* **2010**, *8*, 2756.
[34] J. Seixas de Melo, F. Elisei, C. Gartner, G. G. Aloisi, R. S. Becker, *J. Phys. Chem. A* **2000**, *104*, 6907.
[35] A. Chaieb, L. Vignau, R. Brown, G. Wantz, N. Huby, J. François, C. Dagron-Lartigau, *Opt. Mater.* **2008**, *31*, 68.
[36] A. Chaieb, A. Khoukh, R. Brown, J. François, C. Dagron-Lartigau, *Opt. Mater.* **2007**, *30*, 318.
[37] T. Jiu, Y. Li, H. Gan, Y. Li, H. Liu, S. Wang, W. Zhou, C. Wang, X. Li, X. Liu, D. Zhu, *Tetrahedron* **2007**, *63*, 232.
[38] K. A. Hansford, S. A. P. Guarin, W. G. Skene, W. D. Lubell, *J. Org. Chem.* **2005**, *70*, 7996.
[39] C. C. Wu, M. C. DeLong, Z. V. Vardeny, J. P. Ferraris, *Synth. Met.* **2003**, *137*, 939.
[40] G. P. Bartholomew, X. Bu, G. C. Bazan, *Chem. Mater.* **2000**, *12*, 2311.
[41] A. Bolduc, S. Dufresne, G. S. Hanan, W. G. Skene, *Can. J. Chem.* **2010**, *88*, 236.
[42] S. Dufresne, W. G. Skene, *Acta Cryst.* **2008**, *E64*, o782.
[43] S. Dufresne, W. G. Skene, *Acta Cryst.* **2008**, *E64*, o710.
[44] S. Dufresne, M. Bourgeaux, W. G. Skene, *Acta Cryst.* **2006**, *E62*, o5602.
[45] W. G. Skene, S. Dufresne, T. Trefz, M. Simard, *Acta Cryst.* **2006**, *E62*, o2382.
[46] S. Dufresne, W. G. Skene, *Acta Cryst.* **2010**, *E66*, o3027.
[47] Y. Wang, H. Fu, A. Peng, Y. Zhao, J. Ma, Y. Ma, J. Yao, *Chem. Comm.* **2007**, 1623.
[48] J. Roncali, *Chem. Rev.* **1992**, *92*, 711.
[49] J. r. Heinze, B. A. Frontana-Uribe, S. Ludwigs, *Chem. Rev.* **2010**, *110*, 4724.
[50] M. Bourgeaux, W. G. Skene, *J. Org. Chem.* **2007**, *72*, 8882.
[51] T. Tshibaka, I. Ulliel Roche, S. Dufresne, W. D. Lubell, W. G. Skene, *J. Org. Chem.* **2009**, *74*, 9497.